NANO LETTERS

pubs.acs.org/NanoLett Letter

Bright State Sensitized Triplet Energy Transfer from Quantum Dot to Molecular Acceptor Revealed by Temperature Dependent Energy Transfer Dynamics

Tao Jin, Sheng He, Yifan Zhu, Eilaf Egap, and Tianquan Lian*

Cite This: *Nano Lett.* 2022, 22, 3897−3903 Read Online

ACCESS | Metrics & More | Article Recommendations | Supporting Information

ABSTRACT: Quantum dot (QD) sensitized molecular triplet excited state generation has been a promising alternative for traditional triplet state harvesting schemes. However, the correlation between QD bright/dark states and QD sensitized triplet energy transfer (TET) has been unclear. Herein, we studied the bright/dark states contribution to TET with CdSe/CdS core/shell QD-oligothiophene as the model system. Equilibrium between QD bright and dark states was tuned by changing temperature, and TET dynamics were monitored with transient absorption spectroscopy. Analysis of acceptor triplet excited state growth kinetics yields rates of TET from bright and dark states as 0.492 ± 0.011 ns^{-1} and 0.0271 ± 0.0014 ns^{-1} at 5 K, suggesting significant contribution of bright states to TET. The result was rationalized by bright state wave function components with the same electron/hole spin projections leading to nonzero TET probability. The study provides new insights into QD sensitized TET mechanisms and inspiration for future TET efficiency optimization through QD exciton engineering.

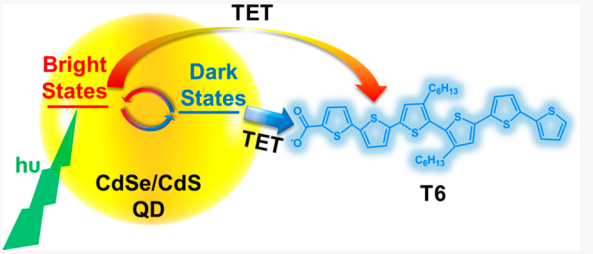

KEYWORDS: *quantum dot, triplet energy transfer, exciton fine structure, transient absorption spectroscopy*

Molecular triplet state generation has received extensive research interest because of its wide applications in photodynamic therapy,[1,2] photon up-conversion[3−5] and photocatalytic organic reactions.[6,7] Traditional approaches for triplet excited state formation include intersystem crossing of target molecules and triplet energy transfer (TET) from molecular sensitizers. Both approaches involve intersystem crossing from singlet excited states generated by light absorption, a process with large energy loss because of the relatively large energy gap between molecular singlet and triplet states.[5] Recently, quantum dot (QD) sensitized TET[8−11] has been developed as a promising route for triplet excited state generation because of the unique advantages of QD sensitizers, including large extinction coefficients,[12,13] tunable absorption from visible to near- and mid-infrared regions,[14,15] and small bright and dark state energy difference.[16,17] So far, TET from QDs to molecular acceptors has been demonstrated for QD sensitizers including CdSe,[18,19] PbS,[20] InP,[21] CdS,[22] and $CsPbBr_3$ perovskite[8] and has been integrated into photon up-conversion[23−26] and photocatalytic organic synthesis.[27,28] The TET mechanisms from QD sensitizers to molecular acceptors have also been studied as it is a key step to determine the overall efficiency of up-conversion or photocatalysis systems.[29] Inspired by TET and other triplet excited state generation schemes in molecular donor−acceptor systems, similar mechanisms have been proposed for TET in QD-acceptor complexes, which include direct TET mediated by charge transfer virtual states[18,30−33] and TET mediated by sequential charge transfer with charge separated state intermediate.[34,35]

While unique properties of QDs have been utilized to improve the TET efficiency of QD-acceptor complexes, their influences on mechanisms of QD sensitized TET have rarely been discussed. Molecule-to-molecule TET through direct Dexter mechanism involves optically forbidden triplet excited states of the donor and acceptor molecules. In QDs, because of strong spin−orbit coupling, spin is no longer a good quantum number and bright and dark exciton states resulted from the bound conduction band (CB) edge electron and valence band (VB) edge hole pair are determined by their total angular momentum. These degenerate bright and dark exciton states are further split by electron−hole exchange and QD shape or lattice asymmetry to form band edge exciton fine structures.[16,36−40] For example, in CdSe QDs with a wurtzite crystal structure, the 2-fold degenerate $1S_{1/2}$ electron level, and 4-fold degenerate $1S_{3/2}$ hole level form 8 exciton states with total

Received: January 4, 2022
Revised: May 8, 2022
Published: May 13, 2022

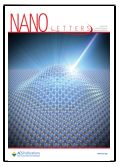

https://doi.org/10.1021/acs.nanolett.2c00017
Nano Lett. 2022, 22, 3897−3903

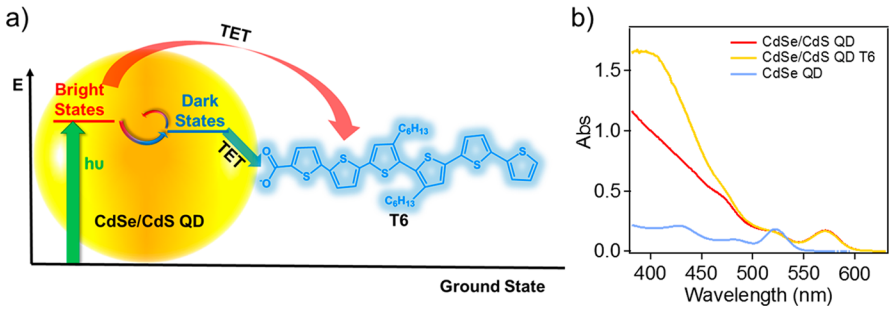

Figure 1. (a) Photophysical processes (arrows) in CdSe/CdS QD-T6 complex following QD excitation. The QD bright state generated by excitation can relax to the dark state, and both bright and dark states can undergo triplet energy transfer (TET) to T6. (b) UV−vis absorption spectra of free CdSe QDs (blue), free CdSe/CdS QDs (red) and CdSe/CdS QD-T6 complexes (yellow) embedded in polymer films at room temperature.

angular momentum of 0, 1, and 2, respectively, which are further split according to their angular momentum projection along the wurtzite hexagonal axis (z axis) to form exciton fine structures with a manifold of bright and dark states spanning an energy range of a few to tens of meVs.[16] These bright and dark states have mixtures of electron spin singlet and triplet characters, and it is unclear and has not been demonstrated experimentally how QD band edge exciton fine structure affects the TET process from the QD sensitizer to molecular acceptors. Such ambiguity in QD sensitized TET mechanisms could impede further optimization of the TET efficiency. Therefore, detailed examination of the effect of exciton fine structure on QD sensitized TET is necessary.

In this work, we systematically tune the relative population of bright and dark states in CdSe/CdS core/shell QDs by varying the temperature and study its effect on the TET dynamics from the QD to attached triplet acceptors with transient absorption (TA) spectroscopy. We use a functionalized oligothiophene (3‴,4″-dihexyl-[2,2′:5′,2″:5″,2‴:5‴,2⁗:5⁗′,2⁗′:5⁗′,2⁗″-sexithiophene]-5-carboxylic acid (T6)) (shown in Figure 1a) as the acceptor following a previous report of efficient TET in CdSe-T6 complexes.[19] With increasing population of dark states at lower temperature, kinetics of triplet excited states of T6 show slower growth. Further kinetics analysis shows that rate of TET from the bright states to T6 is higher than that from the dark states. The bright states contribution to TET can be attributed to the wave function components with triplet-state-like spin characters, resulting in nonzero TET transition probability.

CdSe/CdS core/shell QDs and T6 molecules were synthesized according to procedures from previous literature,[19,41] and the preparations of QD-T6 complexes dispersed in toluene or embedded in a polymer matrix on the surface of glass substrate are described in Supporting Information (SI) Sections SI1 and SI2. CdSe/CdS core/shell QDs instead of bare CdSe QDs were selected as the sensitizer because of their low trap state population, which may also contribute to triplet energy transfer and complicate the analysis.[41,42] The UV−vis absorption spectra of the QD and QD-T6 complexes are shown in Figure 1b. The $1S_h-1S_e$ absorption peak of the QD is centered at 570 nm and shows negligible shift after T6 adsorption. The QD-T6 spectrum shows an additional peak centered at 400 nm due to the T6 S_0-S_1 absorption.[19] It was shown previously that there exists an equilibrium of T6 molecules bound on the QD surface and dissolved in solvent, and the average number of bound T6 per QD for samples prepared under the same condition was estimated to be ~0.5.[19] The surrounding temperature of the QD-T6 complex was tuned by placing the film sample into a Janis STVP-100 cryostat (more details in Section SI1). As shown in Figure S2 in Section SI3, when temperature is decreased from room temperature to 40 K, the $1S_h-1S_e$ exciton peaks of the QD and QD-T6 both blue shift to 550 nm, consistent with previous observations.[43] However, in the temperature regime of 5−40 K, there is a negligible $1S_h-1S_e$ absorption peak shift of QD and QD-T6, indicating a negligible change of the QD to T6 TET driving force in this temperature range.

Thermal equilibrium of bright and dark states in free CdSe/CdS QDs was studied with temperature dependent TA spectroscopy. TA spectra of QDs at room temperature with 550 nm pulse excitation (Figure 2a) show the exciton bleach

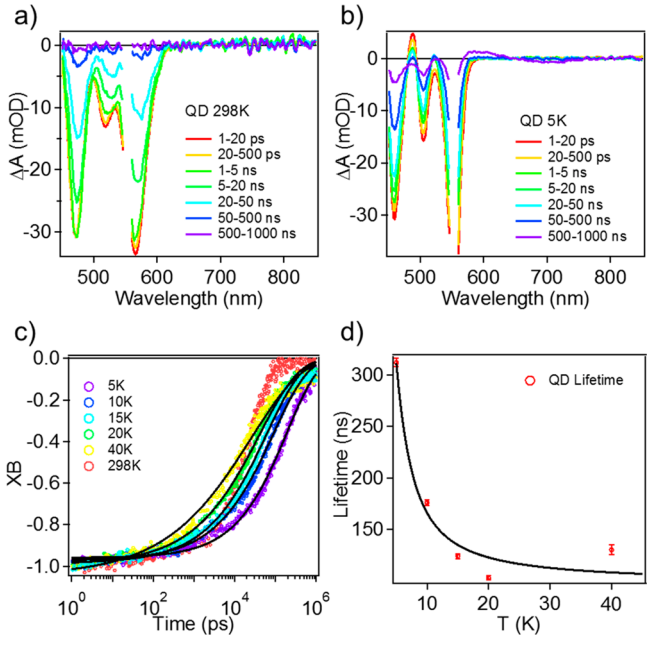

Figure 2. Temperature dependent TA spectra and kinetics of free CdSe/CdS QDs measured with 550 nm pulse excitation. Average TA spectra of QDs at (a) 298 and (b) 5 K at indicated delay time window. (c) Comparison of $1S_h-1S_e$ XB kinetics of QDs at indicated temperatures from 5 to 298 K (open symbols) and their fits to stretched exponential function (black solid lines). (d) Average lifetimes of $1S_h-1S_e$ XB recovery kinetics as a function of temperature (open symbols) and fit to the model of thermal equilibrium between bright and dark states (black solid line). Details of the model are described in the main text.

https://doi.org/10.1021/acs.nanolett.2c00017
Nano Lett. 2022, 22, 3897−3903

(XB) of $1S_h-1S_e$ transition at 570 nm and the transition from higher hole levels to the $1S_e$ level (denoted as the T band) at 473 nm, respectively, similar to previous reports.[44] As temperature decreases from room temperature to 40 K, XB peaks of $1S_h-1S_e$ transition and T band blue shift to ~550 and 459 nm, respectively, along with decrease of the peak line width, as shown in Figure 2b and Figure S3 in Section SI4. In the temperature regime of 5−40 K, the position and line width of the XB peaks show negligible changes. The result is consistent with the QD UV−vis spectra change as a function of temperature and can be rationalized by decreasing lattice expansion and exciton−phonon coupling with decreasing temperature.[43,45,46] As shown in Figure 2c, the $1S_h-1S_e$ XB kinetics show slower decay from 40 to 5 K, which can be attributed to increasing population of dark state with longer lifetime at lower temperature,[47−49] consistent with previous reports of temperature dependent photoluminescence lifetimes of CdSe QDs.[48] Compared to XB kinetics at 40 K, XB kinetics at 298 K shows slower decay from 1 ps to 10 ns and faster decay from 10 ns to 1 μs. The difference is attributed to not only bright−dark state population change but also the change in trap state population from 40 to 298 K.[50−52] For this reason, our analysis is focused on the temperature dependent changes from 40 to 5 K, which can be attributed to changes in bright and dark state populations with negligible effects caused by a change of trap states.[48] Note that XB decay is dominated by decay of bright/dark states to ground states instead of other nonradiative pathways because of the high photoluminescence quantum yield of QD in this temperature regime.[48]

XB kinetics from 5 to 40 K can be well-fit with stretched exponential function, as shown in eq 1.

$$A(t) = A_0 e^{-(t/\tau_k)^{\beta}} \quad (1)$$

In eq 1, $A(t)$ and A_0 are signal amplitudes at time t and $t = 0$, respectively, and τ_k and β are the time constant and stretching exponent of the stretch exponential function. The fitting parameters are listed in Table S1 in Section SI5. Average lifetime of XB kinetics can be calculated from fitting parameters according to

$$\langle\tau\rangle = \frac{\tau_k}{\beta}\Gamma\left(\frac{1}{\beta}\right) \quad (2)$$

where Γ is the gamma function.[53] Average XB decay lifetime as a function of temperature is plotted in Figure 2d. On the basis of a kinetics model involving forward and backward transfer from bright to dark states in QD (more specifically $\pm1^L$ bright states and ±2 dark states) and their decays to ground state,[48] temperature dependent average XB decay lifetime can be fit as

$$\frac{1}{\langle\tau\rangle} = \frac{\frac{1}{\tau_b}e^{-E/kT} + \frac{1}{\tau_d}}{e^{-E/kT} + 1} \quad (3)$$

where $\langle\tau\rangle$ is the average lifetime of XB kinetics; τ_b and τ_d are the decay time constants from bright and dark states to ground state, respectively; E is the energy difference between bright and dark states, and k is the Boltzmann constant. (More details in Section SI5 and Figure S4). Herein, it is assumed that contribution of bright state to XB is as large as that of dark state based on a simplified fine structure model described in Section SI5 and Figure S4. The fitting yields $E = 1.21 \pm 0.55$ meV, $\tau_b = 46.5 \pm 7.0$ ns, and $\tau_d = 486 \pm 117$ ns. The result agrees with findings of temperature dependent QD photoluminescence experiment in previous literature.[47−49,54,55] For example, it has been reported that the dark exciton lifetime decreases from ~1.4 to ~0.3 μs when the CdSe QD diameter increases from 1.7 to 6.3 nm.[48] In summary, equilibrium between bright and dark states ($\pm1^L$ and ±2, respectively) in CdSe/CdS QD can be tuned by temperature.

Temperature dependent TET from CdSe/CdS QDs to attached T6 was studied with TA spectroscopy. Because there is no absorption of T6 at 550 nm (see Figure 1b), QD can be selectively excited with a 550 nm pump−pulse, as confirmed in Section SI6 and Figure S5. As shown in Figure 3a,b and Figure

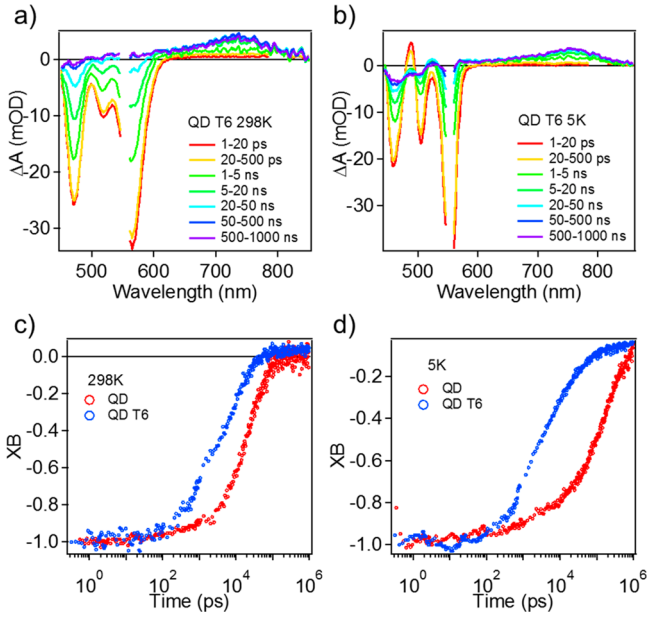

Figure 3. (a and b) TA spectra of QD T6 complex from 1 ps to 1 μs with 550 nm excitation at 298 and 5 K, respectively. (c and d) Comparison of $1S_h-1S_e$ XB kinetics of QD in QD-T6 complex (blue) and in free QD (red) at 298 and 5 K, respectively.

S6 in Section SI7, TA spectra of QD-T6 complexes at all temperatures show the same spectral features as those of free QDs at corresponding temperatures from 1 to 20 ps, indicative of QD exciton generation. The TA spectra show growth of an additional broad positive peak at 600−850 nm due to the T6 T_1-T_n absorption[19] along with decay of the QD XB signal on the 500 ps to 500 ns time scale, indicative of formation of T6 T_1 state (well-defined spin state) by TET from QD. With a temperature decrease from 298 to 40 K, the $T_1 \rightarrow T_n$ peak of T6 shows a slight decrease of maximum peak amplitude and slight red shift with peak maxima from 735 to 755 nm, while negligible peak shift is observed in 5−40 K. The peak shift may be attributed to aggregation of adsorbed T6 molecule at low temperature.[56] The $1S_h-1S_e$ XB signal in QD-T6 complexes recovers faster than free QDs after ~100 ps, as shown in Figures 3c,d and S7, consistent with TET from the QD to T6. XB decay kinetics of QD-T6 complexes is consistent with kinetics of T6 triplet signal growth, as shown in Figure S8, suggesting direct Dexter type TET from QD to T6 without other intermediates. This also agrees with a previous report of direct Dexter type TET from CdSe QDs to adsorbed T6 molecules.[19]

Temperature dependent TET from QD to T6 is further demonstrated in T6 triplet signal growth kinetics extracted

https://doi.org/10.1021/acs.nanolett.2c00017
Nano Lett. 2022, 22, 3897−3903

from TA. The kinetics can be obtained by averaging kinetics from 700 to 800 nm of QD T6 TA spectra and is shown in Figure 4a,b. Because of negligible QD signal amplitude in this

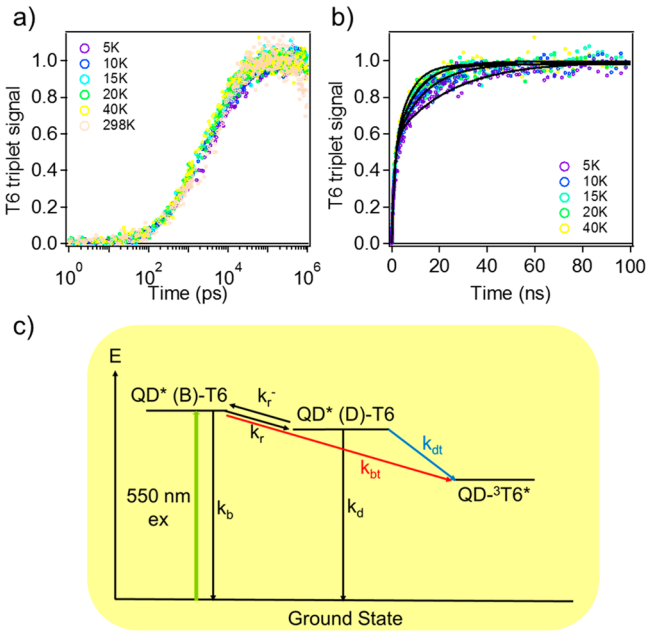

Figure 4. Temperature dependent T6 triplet signal ($T_1 \rightarrow T_n$ induced absorption) growth kinetics and the corresponding kinetics model. (a) T6 triplet signal growth kinetics from 1 ps to 1 μs in temperature regime of 5 K (purple) to 40 K (yellow) and at 298 K (light pink) plotted in log scale. (b) T6 triplet signal growth kinetics from 1 ps to 100 ns in temperature regime of 5−40 K plotted in linear scale. The fitting of the kinetics based on the kinetics model is shown as black solid lines. (c) Kinetics model for fitting the T6 triplet signal growth. The model considers the intrinsic decay of bright ($\pm1^L$) and dark states (±2) of QD to ground state (black arrows), forward and backward transfer from bright state to dark state (black arrows), and TET from bright and dark state to form T6 triplet (red and blue arrows, respectively).

regime, the kinetics solely represents the growth of T6 triplet excited state population. As shown in Figure 4a, T6 triplet state mainly grows from 100 ps to 100 ns and shows a relatively small difference for increasing temperature from 5 to 40 K. The small difference can be better resolved in the kinetics plot in Figure 4b and Figure S9 in Section SI8. The kinetics shows almost no dependence on temperature in the delay time range of 1−5 ns but shows slightly slower T6 triplet growth with decreasing temperature in the delay time range of 10−100 ns. The difference is manifested from 5 to 10 K and is not obvious for higher temperature, coinciding with change of thermal equilibrium between brigh and dark states with temperature. The result is consistent with slower $1S_h-1S_e$ XB decay with increasing temperature (shown in Figure S10 in Section SI8). Therefore, TET from QD to T6 is influenced by temperature and is related to bright and dark states equilibrium. To better rationalize the result, we applied the kinetics model in Figure 4c to fit the T6 triplet growth kinetics. The kinetics model involves intrinsic decay of bright/dark states of QD to ground state, exchange between bright/dark states, and potential TET from both bright and dark states to T6 triplet excited state. Considering the large energy difference between QD exciton and T6 triplet excited states (ΔE = 0.41 eV),[19] at the low applied temperatures, back energy transfer from T6 to QD is neglected. On the basis of the model (with more details in Section SI9), T6 triplet excited state growth can be described as

$$[\mathrm{T}] = N_{\mathrm{B0}}k_{\mathrm{bt}}\left(\frac{B+\lambda_1 e^{\lambda_1 t}-1}{(\lambda_1-\lambda_2)\lambda_1}-\frac{B+\lambda_2 e^{\lambda_2 t}-1}{(\lambda_1-\lambda_2)\lambda_2}\right) + N_{\mathrm{B0}}k_{\mathrm{dt}}\left(\frac{k_{\mathrm{r}}e^{\lambda_1 t}-1}{(\lambda_1-\lambda_2)\lambda_1}-\frac{k_{\mathrm{r}}e^{\lambda_2 t}-1}{(\lambda_1-\lambda_2)\lambda_2}\right) \quad (4a)$$

where

$$B = k_{\mathrm{r}}e^{-E/kT} + k_{\mathrm{d}} + k_{\mathrm{dt}} \quad (4b)$$

N_{B0} is the bright state population at t = 0, and λ_1 and λ_2 ($\lambda_1 > \lambda_2$) are the solutions for the following equation:

$$\lambda^2 + (k_{\mathrm{b}} + k_{\mathrm{bt}} + k_{\mathrm{r}} + k_{\mathrm{d}} + k_{\mathrm{dt}} + k_{\mathrm{r}}e^{-E/kT})\lambda + (k_{\mathrm{b}} + k_{\mathrm{bt}} + k_{\mathrm{r}})(k_{\mathrm{d}} + k_{\mathrm{dt}} + k_{\mathrm{r}}e^{-E/kT}) - k_{\mathrm{r}}{}^2e^{-E/kT} = 0 \quad (4c)$$

Because in the Dexter energy transfer framework, the rate of TET from donor (D) to acceptor (A) follows Fermi's golden rule:

$$k_{\mathrm{TET}} = \frac{2\pi}{\hbar}|V|_{\mathrm{TET}}{}^2\,\mathrm{FCWD} \quad (5)$$

where $|V|_{\mathrm{TET}}$ is the coupling strength and FCWD is the overlap integral of the Franck−Condon weighted density of states.[57] Coupling strength for TET is described by wave function overlap and thus is temperature independent for bright and dark states. FCWD can be described by spectra overlap between $T_1 \rightarrow S_0$ transition of the donor and $S_0 \rightarrow T_1$ transition of the acceptor and is temperature dependent.[57,58] Additional term $u(T)$ was added to the fitting to account for changes of k_{bt} and k_{dt} from 5 to 40 K by change in FCWD as

$$k_{\mathrm{bt\,or\,dt}}(T) = k_{\mathrm{bt\,or\,dt}}(5\,\mathrm{K})\,u(T) = k_{\mathrm{bt\,or\,dt}}(5\,\mathrm{K})\,\frac{\mathrm{FCWD}(T)}{\mathrm{FCWD}(5\,\mathrm{K})} \quad (6)$$

Herein $u(T)$ is assumed to be the same for bright and dark states because of the small energy difference between these states.[16] Figure 4b and Figure S9 show the fitting results, which yield the TET rate from bright states to be 0.492 ± 0.011 ns^{-1}, the TET rate from dark states to be 0.0271 ± 0.0014 ns^{-1} at 5 K, the relaxation rate from bright to dark states to be 0.368 ± 0.016 ns^{-1}, and $u(T)$ to be 1.00, 1.00, 0.99, and 1.04 for T = 10, 15, 20, and 40 K, respectively. The negligible change of FCWD from 5 to 40 K further supports that change in TET growth kinetics is mainly due to change in bright/dark state equilibrium. This is consistent with negligible spectra shift and line broadening for both QD and T6 triplet signal from 5 to 40 K in TA spectra of QD T6 complex, suggesting little change in FCWD with temperature. The bright to dark states relaxation rate obtained from fitting is slower compared to values reported in previous literature, which is attributed to the difference in the QD sizes.[49] It should be noted that because of the distribution of QDs with different numbers of adsorbed T6 molecules, there should also be a distribution of TET rates from bright and dark states from these QDs.[19,26] However, under our experimental conditions, with the estimated average number of adsorbed T6 per QD of ~0.5, the TET signal is dominated by QDs with one adsorbed T6.[19] For simplicity,

https://doi.org/10.1021/acs.nanolett.2c00017
Nano Lett. 2022, 22, 3897−3903

only one TET rate constant from the bright and dark exciton states is used in our fitting model.

The faster TET from QD bright states than from dark states differs significantly from TET between molecular donors and acceptors. As shown in Figure S11 in Section SI9, T6 triplet growth would be faster with decreasing temperature if TET occurs solely from dark states based on the kinetics model, which contradicts the experimental observation. Therefore, current experimental result suggests the significant contribution of TET from bright states of QD to attached acceptor. The nonzero rate of TET from the bright state of QD can be accounted for by evaluating spin characters of bright/dark states in QD and TET rate expressions. With the wave function expressions of doubly degenerate $1S_e$ electron states of CdSe/CdS QD and 4-fold degenerate $1S_{3/2}$ hole states (shown as eqs S8−S10 in Section SI10),[16] the wave functions of 0^L, $\pm1^U$, 0^U, $\pm1^L$, and ±2 states can be calculated by considering the asymmetry of QD shape and lattice and electron−hole exchange interaction and shown as eqs S12a−i, which were demonstrated in previous literature.[16] By separating out the spin wave functions of the electron and hole, exciton states wave functions can be generally written as

$$\begin{aligned}\Psi_X(\mathbf{r_e}, \mathbf{r_h}) = {} & c_X^{(1)}\varphi_X^{(1)}(\mathbf{r_e}, \mathbf{r_h})|\uparrow\rangle_e|\uparrow\rangle_h \\ & + c_X^{(2)}\varphi_X^{(2)}(\mathbf{r_e}, \mathbf{r_h})|\uparrow\rangle_e|\downarrow\rangle_h \\ & + c_X^{(3)}\varphi_X^{(3)}(\mathbf{r_e}, \mathbf{r_h})|\downarrow\rangle_e|\uparrow\rangle_h \\ & + c_X^{(4)}\varphi_X^{(4)}(\mathbf{r_e}, \mathbf{r_h})|\downarrow\rangle_e|\downarrow\rangle_h \end{aligned} \quad (7)$$

where $\varphi_X^{(i)}(\mathbf{r_e},\mathbf{r_h})$ is the part of the wave functions of exciton state X involving real space coordinates and consists of envelope functions and Bloch functions with real space coordinates, and $c_X^{(i)}$ is the corresponding constant. Therefore, specifically for CdSe/CdS QD, all exciton states consist of components with the same and opposite electron/hole spin projections, as shown in Figure 5, although spin of electron

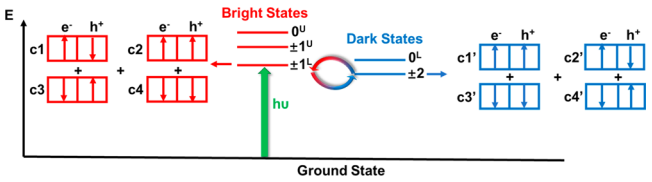

Figure 5. Diagram of bright and dark states in CdSe/CdS QD. The lowest dark states are ±2 states, while the lowest bright states are ±1 states. Wave functions of these states all consist of components with the same and opposite electron/hole spin projections.

and hole in QD is not a good quantum number because of the angular momentum coupling. Note that this characteristic of QD bright/dark state wave functions differs from many molecular sensitizers with well-defined singlet and triplet excited states, but shares some similarity with organometallic sensitizers with strong S_0-T_1 transitions caused by strong spin−orbit coupling.[59−62]

With the wave functions of bright/dark states of QD, the rate of TET from QD can be evaluated. Because of similar FCWD in rates of TET from bright and dark states due to a small energy difference between these states, coupling strength is the factor resulting in the difference of the TET rate of bright and dark states. In Dexter's formula for TET, coupling strength is described as two-electron exchange integral:

$$\begin{aligned}|V| \propto {} & \left\langle \varphi_{HO}^{D}(1)\,\varphi_{LU}^{A}(2)\left|\frac{e^2}{r_{12}}\right|\varphi_{LU}^{D}(2)\,\varphi_{HO}^{A}(1)\right\rangle \\ & \times \langle\chi_{HO}^{D}(1)|\chi_{HO}^{A}(1)\rangle\langle\chi_{LU}^{D}(2)|\chi_{LU}^{A}(2)\rangle \end{aligned} \quad (8)$$

where HO and LU stand for HOMO and LUMO orbitals and χ is the spin wave function (either $|\uparrow\rangle$ or $|\downarrow\rangle$).[57] Equation 8 can be applied to evaluate the exchange integral for TET from QD to T6, with the QD wave function given by eq 7. For example, when considering TET from QD to the triplet excited state of the T6 with the same electron spin projections in HOMO and LUMO ($m_S = \pm1$, in which $S = 1$ is total spin of electrons in T6), the integral in eq 8 will be nonzero only if spin projections of QD electron and hole are the same. Because both bright and dark states contain components with the same electron and hole spin projections, as shown in eq 7 and Figure 5, the TET coupling matrix elements are nonzero for both bright and dark states. The analysis is consistent with experimental results that both bright and dark states of QD can undergo TET to form a T6 triplet excited state. More quantitative evaluation of the relative TET coupling strengths from the bright and dark states is difficult because they are determined by not only the relative contribution of spin triplet components to the QD wave function but also the wave function overlaps between the QD and T6 triplet states. The evaluation of the latter is beyond the scope of this work and would likely require advanced modeling of the wave functions of the QD-T6 complexes. TET pathways with charge transfer virtual states have been considered to outcompete direct Dexter energy transfer described by two-electron exchange integral.[32,63] In this scenario, one-electron integral for electron/hole transfer should be evaluated, in which the same spin integral terms $\langle\chi_{HO}^{D}(1)|\chi_{HO}^{A}(1)\rangle$ and $\langle\chi_{LU}^{D}(2)|\chi_{LU}^{A}(2)\rangle$ will be included. Therefore, the conclusion that bright and dark states both can undergo TET in CdSe/CdS QD is still valid for TET pathways involving virtual states.

In summary, we demonstrate the TET in CdSe/CdS core/shell QD-functionalized oligothiophene complex sensitized by both bright and dark states through analysis of dependence of TET dynamics on temperature, which could shift equilibrium between bright and dark states. Nonzero TET rate of bright and dark states can be rationalized by considering the electron and hole spin projections in wave functions of QD, with components of the same electron/hole spin projections bringing about nonzero TET probability. The conclusion is applicable to various TET pathways involving direct two-electron exchange Dexter energy transfer and charge transfer virtual state mediated TET. Similar analysis may also be applied to other QDs, including PbS and $CsPbBr_3$ QDs. Our finding suggests that simple analogy between bright/dark states in QDs and singlet/triplet excited states in molecules cannot be made, and the mechanisms for QD sensitized TET should be treated differently in certain aspects compared to mechanisms for TET in molecular donor−acceptor complexes.

■ ASSOCIATED CONTENT

Supporting Information

The Supporting Information is available free of charge at https://pubs.acs.org/doi/10.1021/acs.nanolett.2c00017.

Sample preparation and experimental setups, temperature dependent absorption spectra, temperature dependent transient absorption spectra, fitting of

https://doi.org/10.1021/acs.nanolett.2c00017
Nano Lett. 2022, 22, 3897−3903

temperature dependent kinetics, and wave functions of bright and dark states of quantum dot (PDF)

AUTHOR INFORMATION

Corresponding Author

Tianquan Lian − *Department of Chemistry, Emory University, Atlanta, Georgia 30322, United States;* orcid.org/0000-0002-8351-3690; Email: tlian@emory.edu

Authors

Tao Jin − *Department of Chemistry, Emory University, Atlanta, Georgia 30322, United States;* orcid.org/0000-0003-4681-1565

Sheng He − *Department of Chemistry, Emory University, Atlanta, Georgia 30322, United States*

Yifan Zhu − *Department of Materials Science and NanoEngineering, Rice University, Houston, Texas 77005, United States;* orcid.org/0000-0002-9816-5764

Eilaf Egap − *Department of Materials Science and NanoEngineering and Department of Chemical and Biomolecular Engineering, Rice University, Houston, Texas 77005, United States;* orcid.org/0000-0002-6106-5276

Complete contact information is available at: https://pubs.acs.org/10.1021/acs.nanolett.2c00017

Notes

The authors declare no competing financial interest.

ACKNOWLEDGMENTS

T.L. gratefully acknowledge the financial support from the National Science Foundation (Grants CHE-1709182, CHE-1726536, and CHE-2004080).

REFERENCES

(1) Majumdar, P.; Nomula, R.; Zhao, J. Activatable triplet photosensitizers: magic bullets for targeted photodynamic therapy. *J. Mater. Chem. C* **2014**, *2* (30), 5982−5997.

(2) Li, X. S.; Kolemen, S.; Yoon, J.; Akkaya, E. U. Activatable Photosensitizers: Agents for Selective Photodynamic Therapy. *Adv. Funct. Mater.* **2017**, *27* (5), 1604053.

(3) Islangulov, R. R.; Kozlov, D. V.; Castellano, F. N. Low power upconversion using MLCT sensitizers. *Chem. Commun.* **2005**, *30*, 3776−3778.

(4) Zhao, W.; Castellano, F. N. Upconverted Emission from Pyrene and Di-tert-butylpyrene Using Ir(ppy)3 as Triplet Sensitizer. *J. Phys. Chem. A* **2006**, *110* (40), 11440−11445.

(5) Singh-Rachford, T. N.; Castellano, F. N. Photon upconversion based on sensitized triplet−triplet annihilation. *Coord. Chem. Rev.* **2010**, *254* (21−22), 2560−2573.

(6) Kim, T.; McCarver, S. J.; Lee, C.; MacMillan, D. W. C. Sulfonamidation of Aryl and Heteroaryl Halides through Photosensitized Nickel Catalysis. *Angew. Chem., Int. Ed.* **2018**, *57* (13), 3488−3492.

(7) Strieth-Kalthoff, F.; James, M. J.; Teders, M.; Pitzer, L.; Glorius, F. Energy transfer catalysis mediated by visible light: principles, applications, directions. *Chem. Soc. Rev.* **2018**, *47* (19), 7190−7202.

(8) Luo, X.; Lai, R.; Li, Y.; Han, Y.; Liang, G.; Liu, X.; Ding, T.; Wang, J.; Wu, K. Triplet Energy Transfer from CsPbBr3 Nanocrystals Enabled by Quantum Confinement. *J. Am. Chem. Soc.* **2019**, *141* (10), 4186−4190.

(9) Mongin, C.; Garakyaraghi, S.; Razgoniaeva, N.; Zamkov, M.; Castellano, F. N. Direct observation of triplet energy transfer from semiconductor nanocrystals. *Science* **2016**, *351* (6271), 369−372.

(10) Mahboub, M.; Maghsoudiganjeh, H.; Pham, A. M.; Huang, Z. Y.; Tang, M. L. Triplet Energy Transfer from PbS(Se) Nanocrystals to Rubrene: the Relationship between the Upconversion Quantum Yield and Size. *Adv. Funct. Mater.* **2016**, *26* (33), 6091−6097.

(11) Gray, V.; Allardice, J. R.; Zhang, Z.; Dowland, S.; Xiao, J.; Petty, A. J.; Anthony, J. E.; Greenham, N. C.; Rao, A. Direct vs Delayed Triplet Energy Transfer from Organic Semiconductors to Quantum Dots and Implications for Luminescent Harvesting of Triplet Excitons. *ACS Nano* **2020**, *14* (4), 4224−4234.

(12) Yu, W. W.; Qu, L. H.; Guo, W. Z.; Peng, X. G. Experimental determination of the extinction coefficient of CdTe, CdSe, and CdS nanocrystals. *Chem. Mater.* **2003**, *15* (14), 2854−2860.

(13) Cademartiri, L.; Montanari, E.; Calestani, G.; Migliori, A.; Guagliardi, A.; Ozin, G. A. Size-Dependent Extinction Coefficients of PbS Quantum Dots. *J. Am. Chem. Soc.* **2006**, *128* (31), 10337−10346.

(14) Ma, Y.; Zhang, Y.; Yu, W. W. Near infrared emitting quantum dots: synthesis, luminescence properties and applications. *J. Mater. Chem. C* **2019**, *7* (44), 13662−13679.

(15) Hudson, M. H.; Chen, M.; Kamysbayev, V.; Janke, E. M.; Lan, X.; Allan, G.; Delerue, C.; Lee, B.; Guyot-Sionnest, P.; Talapin, D. V. Conduction Band Fine Structure in Colloidal HgTe Quantum Dots. *ACS Nano* **2018**, *12* (9), 9397−9404.

(16) Efros, A. L.; Rosen, M.; Kuno, M.; Nirmal, M.; Norris, D. J.; Bawendi, M. Band-edge exciton in quantum dots of semiconductors with a degenerate valence band: Dark and bright exciton states. *Phys. Rev. B* **1996**, *54* (7), 4843−4856.

(17) Scholes, G. D.; Rumbles, G. Excitons in nanoscale systems. *Nat. Mater.* **2006**, *5* (9), 683−696.

(18) Piland, G. B.; Huang, Z. Y.; Tang, M. L.; Bardeen, C. J. Dynamics of Energy Transfer from CdSe Nanocrystals to Triplet States of Anthracene Ligand Molecules. *J. Phys. Chem. C* **2016**, *120* (11), 5883−5889.

(19) Xu, Z.; Jin, T.; Huang, Y.; Mulla, K.; Evangelista, F. A.; Egap, E.; Lian, T. Direct triplet sensitization of oligothiophene by quantum dots. *Chem. Sci.* **2019**, *10* (24), 6120−6124.

(20) Huang, Z.; Xu, Z.; Mahboub, M.; Li, X.; Taylor, J. W.; Harman, W. H.; Lian, T.; Tang, M. L. PbS/CdS Core-Shell Quantum Dots Suppress Charge Transfer and Enhance Triplet Transfer. *Angew. Chem., Int. Ed.* **2017**, *56* (52), 16583−16587.

(21) Lai, R.; Sang, Y.; Zhao, Y.; Wu, K. Triplet Sensitization and Photon Upconversion Using InP-Based Quantum Dots. *J. Am. Chem. Soc.* **2020**, *142* (47), 19825−19829.

(22) Gray, V.; Xia, P.; Huang, Z.; Moses, E.; Fast, A.; Fishman, D. A.; Vullev, V. I.; Abrahamsson, M.; Moth-Poulsen, K.; Lee Tang, M. CdS/ZnS core-shell nanocrystal photosensitizers for visible to UV upconversion. *Chem. Sci.* **2017**, *8* (8), 5488−5496.

(23) Okumura, K.; Mase, K.; Yanai, N.; Kimizuka, N. Employing Core-Shell Quantum Dots as Triplet Sensitizers for Photon Upconversion. *Chem.—Eur. J.* **2016**, *22* (23), 7721−7726.

(24) Wu, M.; Congreve, D. N.; Wilson, M. W. B.; Jean, J.; Geva, N.; Welborn, M.; Van Voorhis, T.; Bulović, V.; Bawendi, M. G.; Baldo, M. A. Solid-state infrared-to-visible upconversion sensitized by colloidal nanocrystals. *Nat. Photonics* **2016**, *10*, 31−34.

(25) Okumura, K.; Yanai, N.; Kimizuka, N. Visible-to-UV Photon Upconversion Sensitized by Lead Halide Perovskite Nanocrystals. *Chem. Lett.* **2019**, *48* (11), 1347−1350.

(26) Xia, P.; Raulerson, E. K.; Coleman, D.; Gerke, C. S.; Mangolini, L.; Tang, M. L.; Roberts, S. T. Achieving spin-triplet exciton transfer between silicon and molecular acceptors for photon upconversion. *Nat. Chem.* **2020**, *12* (2), 137−144.

(27) Jiang, Y.; Weiss, E. A. Colloidal Quantum Dots as Photocatalysts for Triplet Excited State Reactions of Organic Molecules. *J. Am. Chem. Soc.* **2020**, *142* (36), 15219−15229.

(28) Jiang, Y.; Wang, C.; Rogers, C. R.; Kodaimati, M. S.; Weiss, E. A. Regio- and diastereoselective intermolecular [2 + 2] cycloadditions photocatalysed by quantum dots. *Nat. Chem.* **2019**, *11* (11), 1034−1040.

(29) Xu, Z.; Huang, Z.; Jin, T.; Lian, T.; Tang, M. L. Mechanistic Understanding and Rational Design of Quantum Dot/Mediator Interfaces for Efficient Photon Upconversion. *Acc. Chem. Res.* **2021**, *54* (1), 70−80.

(30) Li, X.; Huang, Z.; Zavala, R.; Tang, M. L. Distance-Dependent Triplet Energy Transfer between CdSe Nanocrystals and Surface Bound Anthracene. *J. Phys. Chem. Lett.* **2016**, *7* (11), 1955−1959.
(31) Luo, X.; Han, Y.; Chen, Z.; Li, Y.; Liang, G.; Liu, X.; Ding, T.; Nie, C.; Wang, M.; Castellano, F. N.; Wu, K. Mechanisms of triplet energy transfer across the inorganic nanocrystal/organic molecule interface. *Nat. Commun.* **2020**, *11* (1), 28.
(32) Harcourt, R. D.; Scholes, G. D.; Ghiggino, K. P. Rate expressions for excitation transfer. II. Electronic considerations of direct and through−configuration exciton resonance interactions. *J. Chem. Phys.* **1994**, *101* (12), 10521−10525.
(33) Bai, S.; Zhang, P.; Beratan, D. N. Predicting Dexter Energy Transfer Interactions from Molecular Orbital Overlaps. *J. Phys. Chem. C* **2020**, *124* (35), 18956−18960.
(34) Luo, X.; Liang, G.; Han, Y.; Li, Y.; Ding, T.; He, S.; Liu, X.; Wu, K. Triplet Energy Transfer from Perovskite Nanocrystals Mediated by Electron Transfer. *J. Am. Chem. Soc.* **2020**, *142* (25), 11270−11278.
(35) Lai, R.; Liu, Y.; Luo, X.; Chen, L.; Han, Y.; Lv, M.; Liang, G.; Chen, J.; Zhang, C.; Di, D.; Scholes, G. D.; Castellano, F. N.; Wu, K. Shallow distance-dependent triplet energy migration mediated by endothermic charge-transfer. *Nat. Commun.* **2021**, *12* (1), 1532.
(36) Becker, M. A.; Vaxenburg, R.; Nedelcu, G.; Sercel, P. C.; Shabaev, A.; Mehl, M. J.; Michopoulos, J. G.; Lambrakos, S. G.; Bernstein, N.; Lyons, J. L.; Stoferle, T.; Mahrt, R. F.; Kovalenko, M. V.; Norris, D. J.; Raino, G.; Efros, A. L. Bright triplet excitons in caesium lead halide perovskites. *Nature* **2018**, *553* (7687), 189−193.
(37) An, J. M.; Franceschetti, A.; Zunger, A. The excitonic exchange splitting and radiative lifetime in PbSe quantum dots. *Nano Lett.* **2007**, *7* (7), 2129−2135.
(38) Kane, R. S.; Cohen, R. E.; Silbey, R. Theoretical Study of the Electronic Structure of PbS Nanoclusters. *J. Phys. Chem.* **1996**, *100* (19), 7928−7932.
(39) Shabaev, A.; Mehl, M. J.; Efros, A. L. Energy band structure of CuInS2 and optical spectra of CuInS2 nanocrystals. *Phys. Rev. B* **2015**, *92* (3), 035431.
(40) Sercel, P. C.; Efros, A. L. Band-Edge Exciton in CdSe and Other II-VI and III-V Compound Semiconductor Nanocrystals - Revisited. *Nano Lett.* **2018**, *18* (7), 4061−4068.
(41) Hanifi, D. A.; Bronstein, N. D.; Koscher, B. A.; Nett, Z.; Swabeck, J. K.; Takano, K.; Schwartzberg, A. M.; Maserati, L.; Vandewal, K.; van de Burgt, Y.; Salleo, A.; Alivisatos, A. P. Redefining near-unity luminescence in quantum dots with photothermal threshold quantum yield. *Science* **2019**, *363* (6432), 1199.
(42) Jin, T.; Lian, T. Trap state mediated triplet energy transfer from CdSe quantum dots to molecular acceptors. *J. Chem. Phys.* **2020**, *153* (7), 074703.
(43) Ortner, G.; Schwab, M.; Bayer, M.; Pässler, R.; Fafard, S.; Wasilewski, Z.; Hawrylak, P.; Forchel, A. Temperature dependence of the excitonic band gap in InxGa1-xAs/GaAs self-assembled quantum dots. *Phys. Rev. B* **2005**, *72* (8), 085328.
(44) Zhu, H.; Song, N.; Rodríguez-Córdoba, W.; Lian, T. Wave Function Engineering for Efficient Extraction of up to Nineteen Electrons from One CdSe/CdS Quasi-Type II Quantum Dot. *J. Am. Chem. Soc.* **2012**, *134* (9), 4250−4257.
(45) Mack, T. G.; Jethi, L.; Kambhampati, P. Temperature Dependence of Emission Line Widths from Semiconductor Nanocrystals Reveals Vibronic Contributions to Line Broadening Processes. *J. Phys. Chem. C* **2017**, *121* (51), 28537−28545.
(46) O'Donnell, K. P.; Chen, X. Temperature dependence of semiconductor band gaps. *Appl. Phys. Lett.* **1991**, *58* (25), 2924−2926.
(47) Labeau, O.; Tamarat, P.; Lounis, B. Temperature dependence of the luminescence lifetime of single CdSe/ZnS quantum dots. *Phys. Rev. Lett.* **2003**, *90* (25), 257404.
(48) de Mello Donegá, C.; Bode, M.; Meijerink, A. Size- and temperature-dependence of exciton lifetimes in CdSe quantum dots. *Phys. Rev. B* **2006**, *74* (8), 085320.
(49) Nirmal, M.; Norris, D. J.; Kuno, M.; Bawendi, M. G.; Efros, A. L.; Rosen, M. Observation of the "Dark exciton" in CdSe quantum dots. *Phys. Rev. Lett.* **1995**, *75* (20), 3728−3731.
(50) Gaponenko, M. S.; Lutich, A. A.; Tolstik, N. A.; Onushchenko, A. A.; Malyarevich, A. M.; Petrov, E. P.; Yumashev, K. V. Temperature-dependent photoluminescence of PbS quantum dots in glass: Evidence of exciton state splitting and carrier trapping. *Phys. Rev. B* **2010**, *82* (12), 125320.
(51) Jones, M.; Lo, S. S.; Scholes, G. D. Quantitative modeling of the role of surface traps in CdSe/CdS/ZnS nanocrystal photoluminescence decay dynamics. *Proc. Natl. Acad. Sci. U. S. A.* **2009**, *106* (9), 3011−6.
(52) Jones, M.; Lo, S. S.; Scholes, G. D. Signatures of Exciton Dynamics and Carrier Trapping in the Time-Resolved Photoluminescence of Colloidal CdSe Nanocrystals. *J. Phys. Chem. C* **2009**, *113* (43), 18632−18642.
(53) Zatryb, G.; Podhorodecki, A.; Misiewicz, J.; Cardin, J.; Gourbilleau, F. On the nature of the stretched exponential photoluminescence decay for silicon nanocrystals. *Nanoscale Res. Lett.* **2011**, *6* (1), 106.
(54) Crooker, S. A.; Barrick, T.; Hollingsworth, J. A.; Klimov, V. I. Multiple temperature regimes of radiative decay in CdSe nanocrystal quantum dots: Intrinsic limits to the dark-exciton lifetime. *Appl. Phys. Lett.* **2003**, *82* (17), 2793−2795.
(55) Kim, D.; Okazaki, K.; Nakayama, M. Temperature dependence of the energy transfer of exciton states in bilayer structures of CdSe/ZnS quantum dots. *Phys. Rev. B* **2009**, *80* (4), 045322.
(56) Jin, T.; Uhlikova, N.; Xu, Z.; Zhu, Y.; Huang, Y.; Egap, E.; Lian, T. Enhanced triplet state generation through radical pair intermediates in BODIPY-quantum dot complexes. *J. Chem. Phys.* **2019**, *151* (24), 241101.
(57) Dexter, D. L. A Theory of Sensitized Luminescence in Solids. *J. Chem. Phys.* **1953**, *21*, 836−850.
(58) Lin, S. H. On the Theory of Non-Radiative Transfer of Electronic Excitation. *Proc. R. Soc. London A* **1973**, *335* (1600), 51−66.
(59) Sasaki, Y.; Amemori, S.; Kouno, H.; Yanai, N.; Kimizuka, N. Near infrared-to-blue photon upconversion by exploiting direct S−T absorption of a molecular sensitizer. *J. Mater. Chem. C* **2017**, *5* (21), 5063−5067.
(60) Sasaki, Y.; Oshikawa, M.; Bharmoria, P.; Kouno, H.; Hayashi-Takagi, A.; Sato, M.; Ajioka, I.; Yanai, N.; Kimizuka, N. Near-Infrared Optogenetic Genome Engineering Based on Photon-Upconversion Hydrogels. *Angew. Chem., Int. Ed.* **2019**, *58* (49), 17827−17833.
(61) Wei, Y.; Zheng, M.; Chen, L.; Zhou, X.; Liu, S. Near-infrared to violet triplet−triplet annihilation fluorescence upconversion of Os(ii) complexes by strong spin-forbidden transition. *Dalton Trans.* **2019**, *48* (31), 11763−11771.
(62) Amemori, S.; Sasaki, Y.; Yanai, N.; Kimizuka, N. Near-Infrared-to-Visible Photon Upconversion Sensitized by a Metal Complex with Spin-Forbidden yet Strong S0−T1 Absorption. *J. Am. Chem. Soc.* **2016**, *138* (28), 8702−8705.
(63) Scholes, G. D.; Harcourt, R. D.; Ghiggino, K. P. Rate expressions for excitation transfer. III. An ab initio study of electronic factors in excitation transfer and exciton resonance interactions. *J. Chem. Phys.* **1995**, *102* (24), 9574−9581.

https://doi.org/10.1021/acs.nanolett.2c00017
Nano Lett. 2022, 22, 3897−3903